Available online at www.sciencedirect.com

SCIENCE DIRECT®

Earth and Planetary Science Letters 234 (2005) 223–234

EPSL

www.elsevier.com/locate/epsl

Magma residence time beneath the Piton de la Fournaise Volcano, Reunion Island, from U-series disequilibria

Olgeir Sigmarsson[a,b,*], Michel Condomines[a,c], Patrick Bachèlery[d]

[a]*Laboratoire Magmas et Volcans, C.N.R.S.- Université Blaise Pascal -O.P.G.C., 5 rue Kessler, 63038 Clermont-Ferrand cedex, France*
[b]*Institute of Earth Sciences, University of Iceland, 101 Reykjavik, Iceland*
[c]*Laboratoire de Dynamique de la Lithosphère, CC 058, Université de Montpellier 2 et CNRS, place Eugène Bataillon, 34095 Montpellier cedex 05, France*
[d]*Département des Sciences de la Terre, Université de la Réunion, 15 av. René Cassin, 97489 Saint-Denis cedex, La Réunion, France*

Received 3 December 2003; received in revised form 29 January 2005; accepted 17 February 2005
Available online 18 April 2005
Editor: E. Bard

Abstract

The U, Th and Ba concentrations, ^{238}U–^{230}Th–^{226}Ra–^{210}Pb and ^{228}Ra –^{232}Th disequilibria have been measured in a suite of basalts and oceanites erupted during the last two millennia at Piton de la Fournaise (Réunion Island, Indian Ocean). Most of the variation in the concentration of all three incompatible elements is due to crystal fractionation or accumulation (and incorporation of olivine xenocrysts in the oceanites), but contamination by hydrothermally altered rocks or secondary minerals might explain significant variations in Ba/Th. Basalts with Th contents lower than 2.25 ppm have only been produced in eruptions outside the Enclos Fouqué caldera, whereas more evolved basalts are predominantly observed close to the summit craters, inside the Enclos caldera and the rift-zones. The samples have almost uniform Th/U of 3.95, identical Th isotope ratios (($^{230}Th/^{232}Th$)=0.934) and, therefore, approximately 20% excess of ^{230}Th over ^{238}U. All analysed samples are in ^{228}Ra–^{232}Th radioactive equilibrium, showing the absence of recent (<30 years) Ra–Th fractionation.

Lava flows erupted inside the Enclos caldera and the rift-zones have $(^{226}Ra/^{230}Th)_0$ varying from 1.18 to 1.34, whereas the basalts from craters outside the Enclos caldera and the rift-zones, in addition to the oceanites and the 1945 basalt, have higher $(^{226}Ra/^{230}Th)_0$ around 1.40. This value is assumed to represent that of the deep magma entering the central plumbing system, beneath the Enclos caldera. The evolution through time of $(^{226}Ra/^{230}Th)_0$ is attributed to alternating episodes of near closed-system evolution in one or several, poorly replenished, deep reservoirs, on timescales of the order of 1000 yr, and episodes of increased re-injection and mixing of the deep magma into older magmas of the previous period. Modelling of such a recent re-injection episode, from 1960 to 1998, suggests a short residence time of about 25 yr and a volume of 0.35 km^3 for the shallow reservoir.

* Corresponding author. Laboratoire Magmas et Volcans, C.N.R.S.- Université Blaise Pascal -O.P.G.C., 5 rue Kessler, 63038 Clermont-Ferrand cedex, France. Tel.: +33 473 346 720.

E-mail addresses: o.sigmarsson@opgc.univ-bpclermont.fr (O. Sigmarsson), condomines@dstu.univ-montp2.fr (M. Condomines), Patrick.Bachelery@univ-reunion.fr (P. Bachèlery).

0012-821X/$ - see front matter
doi:10.1016/j.epsl.2005.02.015

At the time of eruption, $(^{210}Pb/^{226}Ra)_0$ in both oceanites and basalts from the Enclos and rift-zones spans a narrow range with a mean value of 0.68, with the exception of the 1945 basalt which has an unusually low ratio of 0.20. The value of 0.68 can be explained by Rn degassing from the shallow magma chamber on a timescale comparable to that deduced from the evolution of $(^{226}Ra/^{230}Th)_0$ in the 1960–1998 period.

Keywords: U-series disequilibria; magma residence time; magma chamber; Piton de la Fournaise; Reunion Island

1. Introduction

The identification and location of magma chambers beneath active basaltic volcanoes is not always straightforward. Measurable deformation just before and during eruptions indicates a subterranean source of pressure changes, often interpreted to be magma chambers, whereas seismic tomography studies may fail to detect small magma reservoirs. When magma can be dated and transfer-time from the mantle source region to the surface estimated, older magmas must be inferred to have been stored in a magma chamber or pockets en route to the surface. The presence or absence of a magma chamber beneath an active volcano could, therefore, be indicated if magma transfer or residence times are obtainable.

According to the definitions in Condomines et al. [1], transfer time is defined here as the time it takes for a magma to move from a given locality at depth to the surface, whereas magma residence time only applies to the time spent in an open-system magma chamber or reservoir. An age derived from crystals either through trace element diffusion (e.g., [2]) or isochron relationships (e.g., [3]) can be much shorter (microlites) or longer (xenocrysts) than transfer or residence time. The residence times in magma chambers beneath Piton de la Fournaise and Kilauea volcanoes have been inferred from compositional variations in the young basaltic lavas [4,5]. However, the deeper structure of the plumbing system below these volcanoes still remains somewhat obscure. Radioactive disequilibria between short-lived nuclides of the ^{238}U-series can yield magma residence time if the composition of both the young magma and the older magma entering and leaving a reservoir respectively can be measured (e.g., [1,6–9]). Here, we present results on ^{230}Th–^{226}Ra–^{210}Pb and ^{232}Th–^{228}Ra systematics measured in historic and pre-historic lava flows from Piton de la Fournaise volcano on Réunion Island in the Indian Ocean. After a brief discussion about the origin of these disequilibria, it will be shown that the new results most likely indicate the presence of a deep magma chamber from which most magma is supplied to a shallow dyke-and-sill complex before being erupted. Estimates are given for the residence time and volume of the summit reservoir.

2. Short geological overview of Piton de la Fournaise

The structure of Piton de la Fournaise volcano has been thoroughly described by Bachèlery [10] and Lénat and Bachèlery [11]. Here, we only emphasise those structures that are pertinent to the interpretation and discussion of the present results. La Fournaise is a shield volcano with at least three major caldera rims decreasing in age from west to east [12]. The youngest one is the Enclos Fouqué (Fig. 1), a horseshoe-shaped depression open to the east and younger than 3.4 ± 1 ka [13]. The floor of the Enclos Fouqué depression is relatively flat west of a prominent central cone which has two summit craters, Dolomieu and Bory. To the east, the slope of the floor steepens abruptly towards the sea at the limit of the Grandes Pentes. Two rift-zones originate from the central cone, one to the north-east and the other to the south-east, and both of them extend outside the Enclos Fouqué depression down to sea level. A significantly older and most likely a deeper-seated fracture extends from the south-east towards the north-west across the island. This fracture may be a fault inherited from the Indian sea-floor [10]. The surface expression of this structure is characterised by numerous large Strombolian cones, or eccentric craters, of highly variable ages, such as Petit Cratère, Commerson, Piton sous le Gîte and Piton Chisny (Fig. 1).

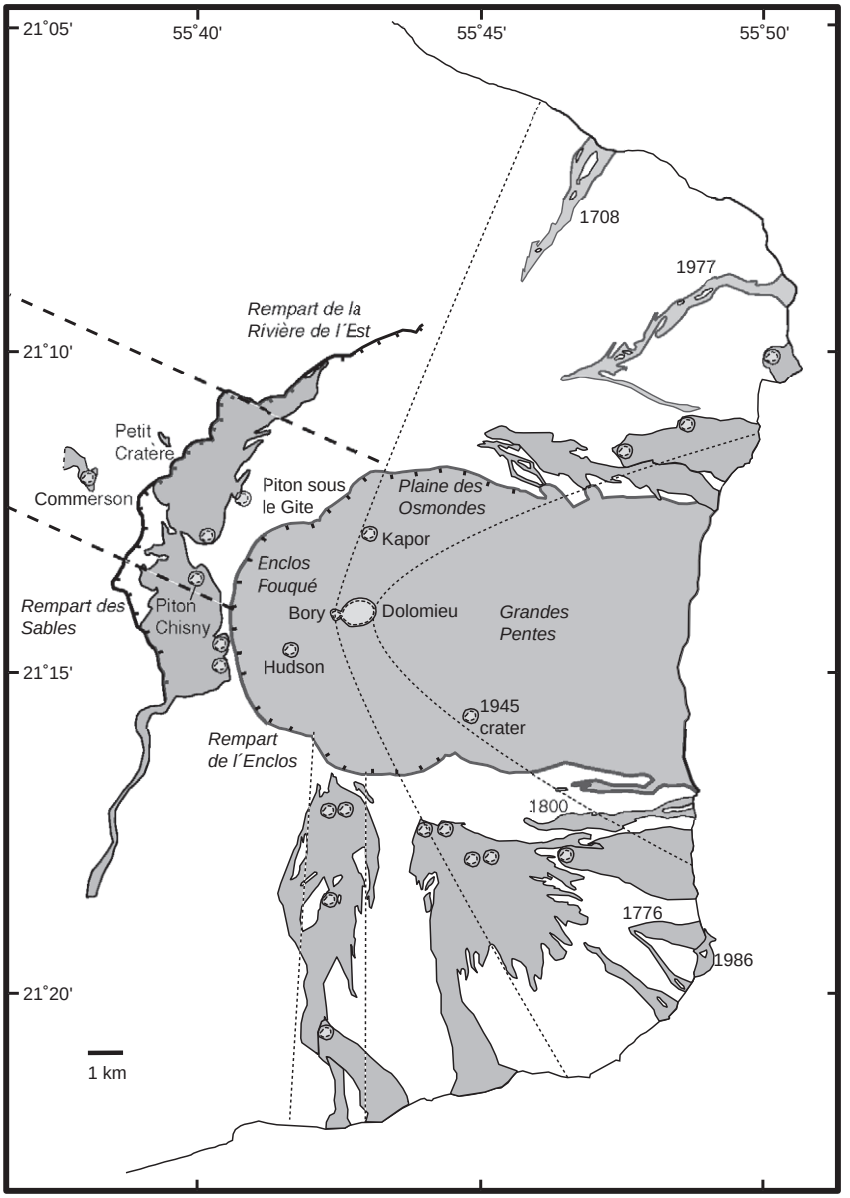

Fig. 1. Simplified map of Piton de la Fournaise showing the two youngest caldera structures, Rempart des Sables and Rempart de la Rivière de l'Est to the west and Rempart de l'Enclos Fouqué marking the depression which opens towards the east. The two rift-zones extending towards SE and NE from the summit craters, and the older N–S rift-zone, south of Enclos [44], are shown with dashed lines. Also displayed is the NW volcanic zone, which is characterised by large eccentric craters and may represent an older fracture zone (see text for discussion). The grey areas represent lava fields younger than the formation approximately 3500 yr ago [13] of the Enclos Fouqué depression.

Since 1980, the volcanic activity of Piton de la Fournaise is being thoroughly monitored by an observatory that has considerably improved the understanding of the pre-eruptive events. The shallow plumbing system is thought to be composed of a dyke-and-sill complex extending from approximately 2.5 km depth towards the surface, above which a hydrothermal system is inferred [11,14]. The recent eruption in 1998 was highly informative and rather unique in the sense that earthquakes originating at

approximately 7 km depth and migrating towards the surface during the last 24 h preceding the eruption were recorded for the first time at Piton de la Fournaise [15]. This depth could correspond to the thickness of the volcanic edifice, beneath which an elongated magma reservoir may be present [16–18].

The basalts produced by Piton de la Fournaise have compositions transitional between tholeiites and alkali basalts and homogeneous Sr and He isotope ratios through the whole history of the volcano (e.g., [19,20] and references therein). Most of the 1998 lavas had compositions similar to those erupted over the preceding decade whereas a small crater, named Hudson, produced lavas with higher MgO. The Hudson lava is thought to represent deeper magma, which is consistent with the presence of olivine phenocrysts having significantly higher forsterite content, and inclusions richer in volatiles [21] compared to other 1998 lavas, such as those from the crater Kapor (Fig. 1). A recent study of fine-scale variations in basalts erupted after 1998 emphasises that small and random crustal contamination may generate subtle but detectable compositional variations [22].

3. Sample selection

In order to estimate melt residence times in magma chambers, the composition of both input and output magmas must be known. Therefore, a special emphasis was placed on collecting ^{14}C-dated prehistoric lava flows from the eccentric craters located NW of the Enclos Fouqué depression [10,23]. Such lavas may have bypassed the central plumbing system and could thus record the composition of the parental magma entering a possible magma chamber beneath Piton de la Fournaise. Our sample suite is therefore not representative of the lava population produced by the volcano, as lavas from the peripheral off-centre craters are over-represented. These samples, which have not been subject to a geochemical study before (Sigmarsson et al., in preparation), are nearly aphyric with only a few olivines visible. An example of such lava comes from the first phase of the Piton Chisny eruption [24]. In contrast, steady-state basalts from inside the Enclos Fouqué and on the rift-zones have up to 15% phenocrysts of olivine, clinopyroxene and plagioclase [10,25]. Still higher crystallinity is observed in the oceanites, or picrites, that may contain 50% of anhedral olivine phenocrysts and/or xenocrysts. They represent basalts that have disrupted and incorporated cumulative olivine (e.g., [20,26]), hence measurements were both performed on whole-rock samples and separated groundmass samples.

Lava from one of the eccentric craters, Petit Cratère, has 18% phenocrysts of olivine, augite and plagioclase displaying skeletal crystal forms that may indicate undercooling and rapid crystallisation of the magma [10]. Several craters on the NW "fracture zone", such as Piton Chisny, erupted mafic and ultramafic xenoliths (e.g., [27]) that suggests fast magma ascent. Finally, the basalt erupted in 1945, at the upper limit of the Grandes Pentes, contains corroded olivine phenocrysts and has a composition intermediate between those of the oceanites and the dominant steady-state basalts [25].

4. Results

Analytical results are given in Table 1 for U, Th, Ra and Ba concentrations as well as the isotope ratios of Th, ^{238}U–^{230}Th–^{226}Ra–^{210}Pb and ^{232}Th–^{228}Ra radioactive disequilibria. The analytical methods employed are described in Condomines et al. [6,28] and Sigmarsson et al. [29,30]. Briefly, the Ba, U and Th concentrations were measured by isotope dilution and thermal ionisation mass spectrometry (TIMS), whereas the ^{226}Ra abundance was either measured by TIMS or by γ-spectrometry. The activities of ^{228}Ra and ^{210}Pb were measured by γ-spectrometry and a few samples were analysed more precisely for ^{210}Pb activities, via α-counting of ^{210}Po, the ^{210}Pb progeny, using a ^{209}Po spike. Analytical uncertainties are discussed in the footnote of Table 1.

4.1. U, Th and Ba concentrations

The concentrations of U, Th and Ba vary by almost a factor of 2 (Fig. 2a,b), the lowest concentrations being found in the oceanites and in a few lavas of the eccentric craters. All three elements behave as incompatible elements, as illustrated in Fig. 2a and b, where the data points plot on straight lines passing through the origin, and their variations are mainly due

Table 1
Analytical results

Sample #	Location	Eruption year	Ba (ppm)	U (ppm)	Th (ppm)	Th/U	$\left(\frac{^{238}U}{^{232}Th}\right)$	$\left(\frac{^{230}Th}{^{232}Th}\right)$	±2σ	$\left(\frac{^{230}Th}{^{238}U}\right)$	(^{226}Ra) (dpm/g)	±2σ	$\left(\frac{^{226}Ra}{^{230}Th}\right)_0$	±2σ	$\left(\frac{^{210}Pb}{^{226}Ra}\right)$	±2σ	$\left(\frac{^{210}Pb}{^{226}Ra}\right)_0$	±2σ	$\left(\frac{^{228}Ra}{^{232}Th}\right)$	±2σ
Oceanites																				
PF77	NE rift-zone	1977	102	0.415	1.67	4.03	0.753				0.538	0.006	1.41	0.033						
PF77 grm	NE rift-zone	1977	154	0.653	2.63	4.03	0.753				0.817	0.01	1.36	0.033	0.834	0.014	0.649	0.029	1.00	0.05
PF1961	Enclos	1961	79.8	0.337	1.33	3.95	0.768				0.398	0.006	1.41	0.034					0.95	0.05
PF1961 grm	Enclos	1961	135	0.581	2.25	3.87	0.784				0.731	0.008	1.42	0.034	0.892	0.022	0.627	0.078		
PF1931 grm	Enclos	1931	144	0.599	2.32	3.87	0.784				0.665	0.006	1.26	0.034	0.966	0.022	0.719	0.178		
Basalts from Enclos and rift zones																				
PF98-3-12W	Hudson	1998	157	0.661	2.60	3.93	0.772				0.793	0.006	1.34	0.033	0.701	0.04	0.692	0.041	1.02	0.04
PF98-3-11	Kapor	1998	138	0.577	2.29	3.97	0.764				0.688	0.006	1.32	0.033	0.732	0.05	0.724	0.052	0.996	0.04
PF90-1-18	Enclos	1990		0.574	2.32	4.04	0.751	0.934	0.011	1.24										
PF88-7-1	Enclos	1989	140	0.581	2.34	4.03	0.753	0.944	0.009	1.25	0.719	0.008	1.33	0.033	0.657	0.08	0.599	0.093	0.999	0.06
PF86-12-52	Enclos	1987	167	0.715	2.85	3.99	0.760													
F2(PF86-3)	SE rift-zone	1986	153	0.643	2.55	3.96	0.766	0.938	0.020	1.22	0.770	0.008	1.32	0.033						
PF86-1-173	Dolomieu	1986	158	0.667	2.65	3.97	0.764	0.939	0.018	1.23	0.808	0.008	1.33	0.033	0.838	0.023	0.750	0.036		
PF1979	Enclos	1979	155	0.709	2.81	3.96	0.766				0.817	0.008	1.27	0.033	0.80	0.05	0.661	0.085		
PF1964	Enclos	1964	166	0.728	2.87	3.94	0.770				0.800	0.007	1.22	0.034	0.897	0.025	0.685	0.075		
PF1945	Enclos	1945	117	0.488	1.86	3.82	0.795				0.606	0.009	1.43	0.034	0.860	0.014	0.200	0.08		
PF1927	Enclos	1927	165	0.633	2.52	3.97	0.764				0.697	0.008	1.23	0.034						
PF1915	Enclos	1915		0.565	2.24	3.97	0.765				0.637	0.006	1.25	0.034						
PF1800	SE rift-zone	1800	127	0.505	1.97	3.90	0.778	0.930	0.009	1.20	0.570	0.007	1.28	0.036						
PF1776	SE rift-zone	1776	137	0.550	2.08	3.78	0.802				0.615	0.006	1.34	0.036						
PF1708	NE rift-zone	1708	147	0.588	2.29	3.89	0.780	0.923	0.008	1.18	0.650	0.006	1.29	0.037						
PF-2	S rift-zone	1600	181	0.712	2.90	4.07	0.745				0.769	0.005	1.20	0.041						
S42	S rift-zone	1340		0.727	2.95	4.06	0.747	0.916	0.007	1.23	0.786	0.006	1.25	0.044						
Basalts from eccentric craters																				
P141	Petit Cratère	1440	109	0.470	1.80	3.84	0.790	0.944	0.005	1.19	0.548	0.005	1.41	0.042						
F23	Chisny	960	144	0.587	2.27	3.89	0.780	0.930	0.020	1.20	0.639	0.008	1.40	0.052						
PF-16	Piton Gîte	600	162	0.635	2.52	3.97	0.765				0.680	0.006	1.33	0.061						
PF-8	Commerson	120	168	0.690	2.80	4.05	0.749				0.729	0.005	1.32	0.075						

Sample coordinates are given in Appendix A. Olivine pheno- and xenocrysts were separated from the three oceanites and listed results are on the groundmass (samples marked grm). Eruption dates are listed as AD. Samples older than 18th century have been dated by 14C and calibrated ages were calculated with the method of Stuiver et al. [43]. Abundance of elements is given in part per million except for Ra, which is listed as disintegration per minute per gram. Parentheses around nuclides denote activity. Analytical errors are approximately 1% for Ba and 0.5% for U and Th contents, and listed errors are internal 2σ uncertainties based on counting statistics or 2SE from mass spectrometry. A few replicate measurements yield 0.5–2% reproducibility for ^{226}Ra and ^{210}Pb activity. The relatively large uncertainties on (^{226}Ra/^{230}Th)$_0$ in prehistoric samples are due to propagated errors of the age determination. The (^{226}Ra/^{230}Th)$_0$ was calculated from the average (^{230}Th/^{232}Th) of 0.934 for samples in which Th isotopes were not measured. The activity of ^{210}Pb was measured either directly by γ-spectrometry or α-spectrometry of ^{210}Po, the ^{210}Pb progeny. The (^{210}Pb/^{226}Ra)$_0$ has been corrected for ^{210}Pb decay during the time elapsed between eruption and analysis.

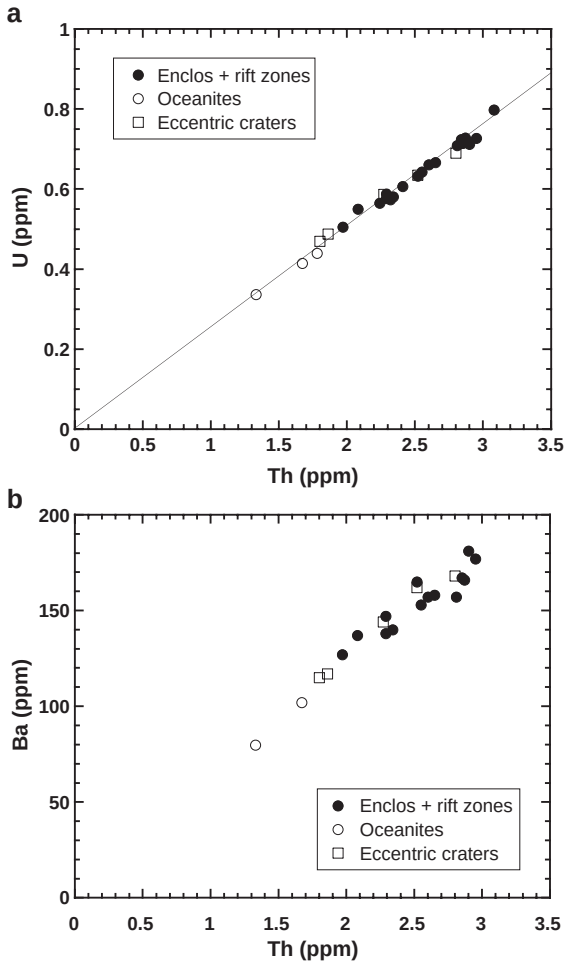

Fig. 2. (a) Linear correlation between U and Th concentrations (R^2=0.987) in recent lavas from Piton de la Fournaise. Due to sampling strategy, compositions of peripheral lavas are over represented in this diagram. In this figure and Fig. 4, the basalt from the peculiar 1945 eruption is plotted with the same symbol (open square) as the basalts from eccentric craters. Most of the variation is assigned to the fractionation, accumulation and possibly dissolution of crystals. The incorporation of olivine xenocrysts explains the much lower U and Th concentrations of the oceanites, and of a few basalts erupted outside Enclos Fouqué near sea level. (b) Concentrations of Ba vs. Th in recent lavas from Piton de la Fournaise (R^2=0.945). The larger scatter in this diagram compared to the U–Th diagram (a) is attributed to shallow contamination by hydrothermally altered rocks or secondary hydrothermal minerals.

to crystal fractionation, accumulation and, possibly, dissolution. Basalts with Th lower than 2.25 ppm have only been produced in lateral eruptions in the rift-zones or from eccentric craters, with the exception of the 1945 basalt, whereas more evolved basalts are predominantly observed close to the summit, inside the Enclos caldera. The lower Th concentration in lavas from the eccentric craters and the 1945 eruption may indicate that more primitive magmas of deeper origin can bypass the central plumbing system. The 1945 eruption site is located at the top of the Grandes Pentes (Fig. 1), where a drastic increase in topographic slope occurs, which has been taken to indicate a deep-seated caldera fault [10]. Furthermore, the Petit Cratère, which is situated on the Rempart des Sables caldera scarp, produced lava with very similar Th concentration as the 1945 lava (1.80 and 1.86, respectively). The oceanites display even lower Th contents, which most likely reflect a dilution effect due to incorporation of xenocrystic olivine. The low Th concentrations in lavas from the low-lying 1776 and 1800 lateral eruptions are explained in a similar manner. In detail, however, whereas the Th/U show only limited variations (around 7%, from 3.78 to 4.07, with a mean value of 3.95 ± 0.03, 2SE, n=26), the Ba/Th covers a larger range, with a 17% variation from 55.9 to 65.9, well outside the analytical uncertainties. The latter ratio correlates neither with the Th abundance nor the U/Th value. These variations will be discussed in the following sections.

4.2. ^{228}Ra–^{232}Th disequilibria

Lava flows at Piton de la Fournaise that are less than 10 yr old are in ^{228}Ra–^{232}Th radioactive equilibrium, suggesting that no fractionation between Th and Ra has occurred during the last 30 yr. Shallow crystallisation, degassing and potential interaction with hydrothermally altered crust beneath Piton de la Fournaise have thus not significantly fractionated Ra from Th.

4.3. ^{238}U-series disequilibria

The activity ratio (^{230}Th/^{232}Th) was measured in 10 samples and is nearly constant within analytical uncertainties, having a mean value of 0.934 ± 0.018. As Th/U is also almost constant, this results in a nearly uniform 22% excess of ^{230}Th over ^{238}U. These values are very similar to the Th/U and (^{230}Th/^{232}Th)$_o$ initial values for ancient lava flows produced by this volcano during the last 300,000 yr [1,31].

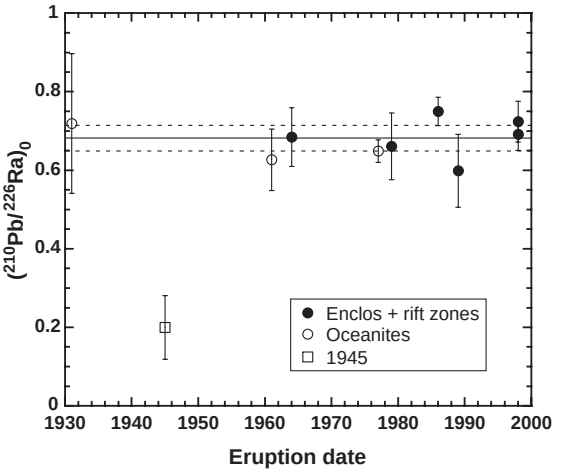

Fig. 3. $(^{210}Pb/^{226}Ra)_0$ values (recalculated to the time of eruption) in lavas erupted during the period 1930 to 1998 AD. With the exception of the 1945 lava, all samples have a mean ratio of 0.68 ± 0.03.

The $(^{226}Ra/^{230}Th)_0$ (ratios recalculated at the time of eruption) vary from 1.18 to 1.43. It should be noted that the highest values, around 1.4, are only found in lavas from eccentric craters (Petit Cratère and Chisny; see map in Fig. 1), the 1945 eruption and in the two youngest oceanites. All the basalts from inside the Enclos Fouqué depression (with the exception of the 1945 lava flow), and those from the rift-zones have lower $(^{226}Ra/^{230}Th)_0$ ratios.

Large deficits of ^{210}Pb relative to ^{226}Ra are observed in all analysed samples (erupted during the last 70 yr). The $(^{210}Pb/^{226}Ra)_0$ (at the time of eruption) are nearly constant, with a mean value of 0.68 ± 0.03 (Fig. 3). A notable exception is the lava from the 1945 eruption, which has a very low $(^{210}Pb/^{226}Ra)_0$ of 0.20 (± 0.08).

5. Discussion

5.1. ^{230}Th–^{238}U disequilibria

Taken together with other published isotope data, such as $^{87}Sr/^{86}Sr$ and $^{3}He/^{4}He$ (0.70403–0.70426 and 12.6–13.6 (R/Ra), respectively; [19,20,25,32,33]), the constant $(^{230}Th/^{232}Th)$ and $(^{230}Th/^{238}U)$ (this study and [1,31]) suggest that the Piton de la Fournaise magmas are derived from a relatively homogeneous mantle source. Moreover, both the extent of melting and the melting processes appear to have remained unchanged at least during the last 300 ka.

5.2. ^{226}Ra–^{230}Th disequilibria

Because ^{226}Ra has a half-life (1600 yr) commensurate with magma transfer or residence times in some active basaltic or andesitic volcanoes (e.g., [1]), ^{226}Ra–^{230}Th disequilibria can potentially provide useful insights into magma dynamics beneath Piton de la Fournaise. However, for that purpose, the processes, other than radioactive decay, that are able to fractionate Ra from Th during magma evolution must first be discussed. It is a common practice to look at the behaviour of Ba, assumed to be a relatively close analogue of Ra during differentiation (even if theoretical studies indicate that Ra should be more incompatible than Ba in major basaltic minerals, e.g., [34]). We have reported in Fig. 4a the Ba/Th against the eruption ages. As already mentioned, significant variations are apparent: in particular, the Ba/Th of the lavas erupted after 1945 tend to be lower than those of the previous eruptions. These variations are difficult to explain by crystal fractionation since they are not correlated with Th contents. Among the major crystallising phases, plagioclase is the only one able to incorporate Ba, and fractionation or accumulation of plagioclase could potentially explain the variations in Ba/Th. However, petrological and geochemical evidence, like the absence of a Eu anomaly [10,25] rules out this possibility. Other explanations include variations in the mantle sources, the degree or dynamics of melting or contamination during magma ascent towards the surface. Although slight variations in mantle sources or melting degrees are possible, they are unlikely to explain the 17% variation in Ba/Th observed among the steady-state basalts erupted inside the Enclos caldera and the rift-zones. Besides their rather uniform major-element composition, these basalts have nearly constant Th/U and $(^{230}Th/^{238}U)$ (this is especially true for basalts erupted during the last century, which display large variations in their Ba/Th). In a recent study of the lavas from the 1998–2002 period, Vlastélic et al. [22] argue that crustal contamination processes explain trace element and Pb isotope variations. The assimilation of hydrothermally altered basalts either in the oceanic crust or within the

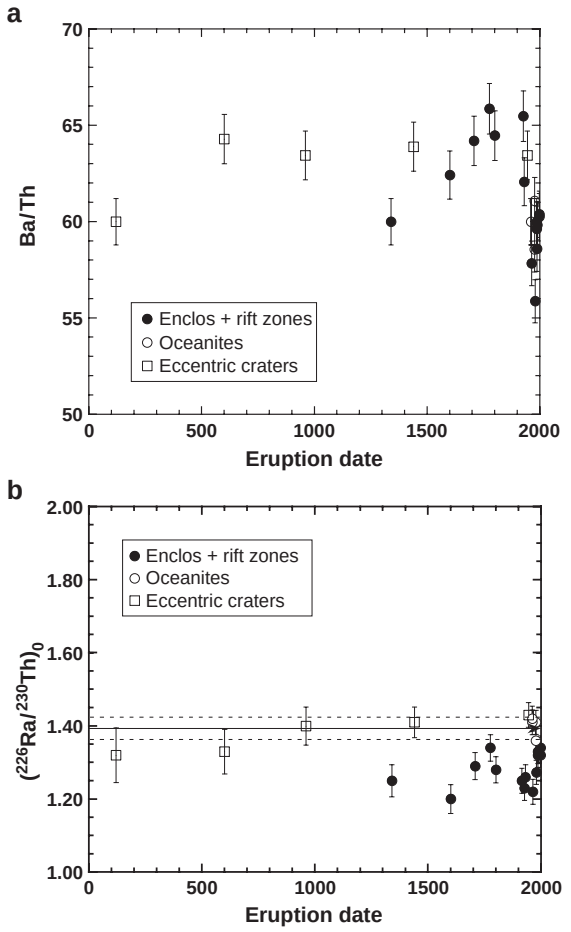

Fig. 4. (a) Ba/Th plotted as function of eruption dates. Note the absence of systematic differences between the ratios of Enclos and rift-zone basalts, and those of oceanites or basalts from eccentric craters (see text for discussion). (b) $(^{226}Ra/^{230}Th)_0$ vs. eruption dates. Basalts from eccentric craters and oceanites have higher ratios (~1.40) than basalts from Enclos and rift-zones. The variations in $(^{226}Ra/^{230}Th)_0$ of the latter are interpreted by alternating periods of near closed-system evolution and episodes of active reinjection (e.g., from 1960 to 1998) of a deep magma with a $(^{226}Ra/^{230}Th)_0$ similar to that of the basalts from the eccentric craters. The horizontal line indicates the average $(^{226}Ra/^{230}Th)_0$ value of oceanites and basalts from eccentric craters (1.40 ± 0.03) (see text for further discussion).

volcanic edifice can indeed affect Ba/Th, especially if secondary minerals like barite are involved during this process. If the altered rocks or secondary minerals are old enough, this contamination will have little effect on the Ra activities. We suggest that most of the variation in Ba/Th can be ascribed to crustal contamination, most likely occurring in-between the dykes and sills beneath the summit craters and through which the majority of the magmas migrate on their way to the surface. An important observation is the lack of systematic differences in Ba/Th of Enclos and rift-zone basalts and those of oceanites and basalts from eccentric eruptions (Fig. 4a).

In contrast, there is a systematic difference between the $(^{226}Ra/^{230}Th)_0$ of oceanites and eccentric basalts, and those of Enclos and rift-zone basalts (Fig. 4b). With the possible exception of the 120 AD Commerson and 600 AD Piton sous le Gîte eccentric eruption, all other oceanites and eccentric basalts have higher $(^{226}Ra/^{230}Th)_0$ (~1.40) than steady-state basalts (from 1.18 to 1.34). This strongly suggests that the differences in $(^{226}Ra/^{230}Th)_0$ can be explained by radioactive decay of the Ra excess in the magma giving rise to the steady-state basalts during magma storage in the central plumbing system, whereas magmas erupted through eccentric craters may have bypassed the central reservoir. These magmas which often contain ultramafic nodules [10] would then have a much shorter transfer time, and their $(^{226}Ra/^{230}Th)_0$ would be little affected and could represent the value of the deep magma entering the reservoir beneath the Enclos caldera. Such a model is similar to the one advocated for Mt Etna by Condomines et al. [1,6]. The situation at Piton de la Fournaise appears a little more complex, however, as the open-system reservoir does not have a constant, steady-state $(^{226}Ra/^{230}Th)$ ratio. Though relatively limited, the variations in $(^{226}Ra/^{230}Th)_0$ of the Enclos and rift-zone basalts are nevertheless significant (Fig. 4b). The observed trend suggests relatively low $(^{226}Ra/^{230}Th)_0$ ratios with a minimum of 1.20 in 1600 AD, followed by an increase up to 1.34 until 1776 AD, a new decrease until 1960 AD and finally an increase from 1960 to 1998 AD. The evolution of the $(^{226}Ra/^{230}Th)_0$ suggests the existence of at least two periods of enhanced reinjection of a deep magma with $(^{226}Ra/^{230}Th)_0$ close to 1.4 (value of the basalt from the eccentric craters) into one or several magma reservoirs filled with "older" magmas whose $(^{226}Ra/^{230}Th)_0$ have been lowered by radioactive decay. An example of magma resulting from such a mixing process could be the 1998 Hudson lava that clearly has a deep origin [22] but a $(^{226}Ra/^{230}Th)_0$ intermediate between the values of the eccentric craters and the summit lavas. This concurs with variable

Fo-contents and high but heterogeneous CO_2 concentrations in olivine melt inclusions of the Hudson basalt [21]. If we attribute the low $(^{226}Ra/^{230}Th)_0$ to radioactive decay during magma storage in the crust, then this storage time should be of the order of 10^3 yr. For example, a decrease from 1.40 to 1.20 would result from 1600 yr of closed-system evolution. However, a detailed interpretation is precluded by the fact that many more eruptions than those studied here occurred during the past centuries. Similar timescales have been proposed for some basalts from Karthala volcano (Grande Comore, Indian Ocean), and for several tholeiitic basalts erupted during the 1978 Ardoukoba eruption (Asal rift, East Africa) [8,35]. Whether this storage time corresponds to the time spent by the magmas in a single reservoir beneath the Enclos caldera or in several magma chambers is difficult to ascertain.

Several lines of evidence suggest the presence of a magma reservoir at about 7 km depth beneath the volcano [15,36]. This depth could correspond to the interface of the volcanic edifice and the older Indian Ocean floor [16,17], which most likely presents a rheological barrier at which a magma reservoir could have developed. Moreover, Aki and Ferrazzini [18] suggest that several "long-period" seismic events may result from vibrations in an elongated magma reservoir at 7 km depth beneath the rift-zones inside the Enclos Fouqué depression. Another smaller storage zone is thought to be composed of a dyke-and-sill complex extending from approximately 2.5 km depth towards the surface [11,39].

In our interpretation–that the episodes of increasing $(^{226}Ra/^{230}Th)_0$ (Fig. 4b) are due to the progressive reinjection and mixing of the deep magma into an older one–it may be possible to deduce the residence time of the magma and thus the volume of the "reservoir" where this process takes place. We have modelled the evolution of $(^{226}Ra/^{230}Th)_0$ during the 1960–1998 period following the simple model proposed by [28] for a reservoir of constant volume. On such a short timescale, both ^{226}Ra and ^{230}Th can be considered as stable elements. The parameters used in the calculations are given in the caption of Fig. 5. The evolution of the $(^{226}Ra/^{230}Th)_0$ can be explained if the residence time τ is around 25 yr. This estimate is similar to the 14 to 43 yr suggested by Albarède [4,37]. They are also comparable to the residence times of 30–40 yr for the late 20th century in the shallow reservoir beneath Kilauea summit [4], despite significantly higher magma supply rates at Hawaii.

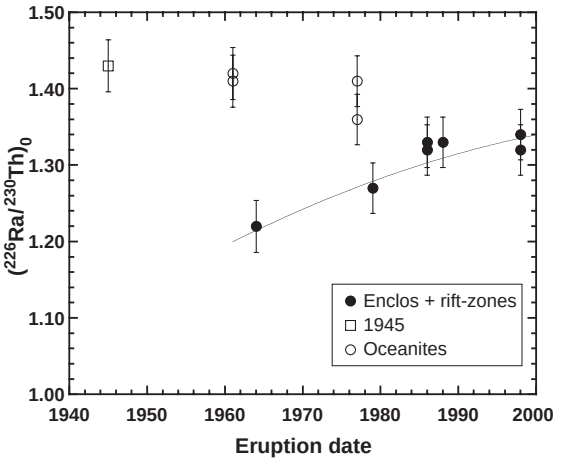

Fig. 5. Detailed modelling of the 1960–1998 reinjection episode. On such a timescale, both ^{226}Ra and ^{230}Th are considered as stable elements. The equation describing the evolution of the concentration of a stable element vs. time in this process of progressive injection and mixing in a magma chamber of constant volume is: $C = C_i.\ (1 - e^{-t/\tau}) + C_0 \cdot e^{-t/\tau}$ (from [28] where the parameter ν is replaced here by $1/\tau$). C_i and C_0 are the concentrations in the injected and initial resident magma, respectively, and τ is the magma residence time. The curve shown in the diagram corresponds to the following parameters: $[Th]_i$ and $[Th]_0 = 1.80$ and 2.90 ppm, respectively (cf. Table 1 and Fig. 2a), $(^{226}Ra/^{230}Th)_i$ and $(^{226}Ra/^{230}Th)_0 = 1.40$ and 1.20, respectively, and $\tau = 25$ yr. The reinjection process is assumed to have begun in 1961, after the oceanite eruption.

The volume of the reservoir $V = \phi * \tau$ is easily calculated if the flux of magma entering or leaving the reservoir, ϕ, can be estimated. The output rate is the sum of the magma extrusion and intrusion rates. The average lava production rate during the 20th century is close to 0.34 m^3/s [38–40] and around 0.40 m^3/s since 1977, or 0.011–0.013 km^3/yr. The volume of magma left as intrusions is at least 13% [41] of the volcanic edifice. The output rate would, thus, be closer to 0.014 km^3/yr, which results in a reservoir volume of about 0.35 km^3. This small volume is unlikely to correspond to the deep reservoir described above: it could represent only the "active" part of this reservoir, or a smaller magma chamber at a shallower depth, in which the mixing between the "old" magma and the new inflowing magma takes place.

The occurrence in the Enclos caldera and the rift-zones of episodic oceanite eruptions, with high $(^{226}Ra/^{230}Th)_0$ similar to those of the eccentric basalts, suggests that these magmas have escaped mixing with older magma on their way towards the surface. This could be due to a complex geometry of the plumbing system or simply to the fact that the high flow rate of these magmas in the crust has prevented efficient mixing with the resident magma.

5.3. ^{210}Pb–^{226}Ra disequilibria

The $(^{210}Pb/^{226}Ra)_0$ values are plotted vs. eruption dates in Fig. 3. With the notable exception of the 1945 basalt, all other basalts erupted inside the Enclos and rift-zones, as well as the two oceanites from the 1931 and 1977 eruptions display a narrow range of $(^{210}Pb/^{226}Ra)_0$, with a mean value of 0.68 ± 0.03. A $(^{210}Pb/^{226}Ra)_0$ lower than 1 might result from ^{222}Rn degassing in shallow magma chambers, as modelled by Gauthier and Condomines [42] for closed and open-system reservoirs. When the Piton de la Fournaise magma enters the dyke-and-sill complex that has been inferred at approximately 2500 m depth, vigorous degassing of H_2O is expected, and this will carry Rn atoms upwards. According to the model above, a $(^{210}Pb/^{226}Ra)_0$ of 0.68 would be reached after about 12 yr of continuous Rn degassing in a non-renewed reservoir (assuming 100% Rn loss, and an initial $(^{210}Pb/^{226}Ra)_0$ of 1). It would take longer time to attain this value in a renewed magma chamber or if the Rn loss is incomplete. A detailed discussion of these ratios is difficult because several other processes might well fractionate Pb and Ra, in addition to Rn degassing. This is suggested by the very low value of the 1945 basalt. If that low value only resulted from continuous Rn degassing in a non-renewed reservoir, the storage time would have to be about 50 yr at shallow level. In view of the rather primitive character of the 1945 basalt, and its $(^{226}Ra/^{230}Th)$ identical to those of the oceanites and basalts from eccentric craters, this rather long storage time appears unlikely. Other processes like iron sulphide precipitation at depth or Pb volatilisation during the eruption could explain such a low value. It is also difficult to advocate only Rn degassing in a shallow reservoir to explain the $(^{210}Pb/^{226}Ra)_0$ of the 1931, 1961 and 1977 oceanites, similar to those of the Enclos and rift-zone basalts. One would expect $(^{210}Pb/^{226}Ra)_0$ closer to 1 for these deep, less degassed magmas. Clearly, a detailed interpretation of $(^{210}Pb/^{226}Ra)_0$ would require more data on Pb behaviour during magma differentiation.

6. Conclusion

The interpretation of ^{226}Ra–^{230}Th disequilibria in a suite of basalts erupted during the last two millennia at Piton de la Fournaise suggests that some magmas showing low $(^{226}Ra/^{230}Th)_0$ might have resided for about 1500 yr in one or several deep reservoirs. The variations of these ratios through time in basalts erupted in the Enclos and the rift-zones probably result from alternating episodes of more or less closed-system evolution and episodes of increased reinjection of a deep magma with a higher $(^{226}Ra/^{230}Th)_0$ ratio. This latter magma is best represented by lavas erupted through eccentric craters, which bypass the central reservoir(s) and thus escape mixing with "older" magmas in the central plumbing system, and by oceanites, whose high flow rate in the crust prevents their effective mixing with the old resident magmas beneath the Enclos caldera. The modelling of the most recent reinjection episode (1960–1998) suggests a magma residence time of about 25 yr, and a volume of 0.35 km^3 for the shallow reservoir. A more complete interpretation of geochemical results should take into account the complexity of the plumbing system, which is only possible through a detailed study of all recently erupted lavas and of the relationships between geochemical, volcanological and geophysical data (effusion rate, volatile contents, seismic signals...).

Acknowledgements

This research was in part supported by the Commission of the European Communities in the framework of European Laboratory Volcanoes and the French PNRN programme of INSU-CNRS. We are grateful to Chantal Bosq and Karin David for their help with the Ba analysis. We would also like to acknowledge input from Jean-François Lénat and Ariel Provost as well as animated discussions with

Françis Albarède. Constructive reviews by P.Y. Gillot, S.J. Goldstein and K.W. Sims helped improve the paper. Discussions and corrections of the English by S. Steinthorsson were much appreciated.

Appendix A. Supplementary data

Supplementary data associated with this article can be found, in the online version, at doi:10.1016/j.epsl.2005.02.015.

References

[1] M. Condomines, P.-J. Gauthier, O. Sigmarsson, Timescales of magma chamber processes and dating of young volcanic rocks, Rev. Mineral. Geochem. 52 (2003) 125–174.
[2] G.F. Zellmer, S. Blake, D. Vance, C. Hawkesworth, S. Turner, Plagioclase residence times at two arc volcanoes (Kameni Islands, Santorini and Soufriere, St. Vincent) determined by Sr diffusion systematics, Contrib. Mineral. Petrol. 136 (1999) 345–357.
[3] K.M. Cooper, M.R. Reid, M.T. Murrell, D.A. Clague, Crystal and magma residence time at Kilauea Volcano, Hawaii: ^{230}Th–^{226}Ra dating of the 1955 East Rift eruption, Earth Planet. Sci. Lett. 184 (2001) 703–718.
[4] F. Albarède, Residence time analysis of geochemical fluctuations in volcanic series, Geochim. Cosmochim. Acta 57 (1993) 615–621.
[5] A.J. Pietruszka, M.O. Garcia, The size and shape of Kilauea Volcano's summit magma storage reservoir: a geochemical probe, Earth Planet. Sci. Lett. 112 (1992) 61–73.
[6] M. Condomines, J.-C. Tanguy, V. Michaud, Magma dynamics at Mt. Etna: constraints from U–Th–Ra–Pb radioactive disequilibria and Sr isotopes in historical lavas, Earth Planet. Sci. Lett. 132 (1995) 25–41.
[7] O. Sigmarsson, Short magma chamber residence time at an Icelandic volcano inferred from U-series disequilibria, Nature 382 (1996) 440–442.
[8] N. Vigier, B. Bourdon, J.L. Joron, C.J. Allègre, U-decay series and trace element systematics in the 1978 eruption of Ardoukoba, Asal rift: timescale of magma crystallization, Earth Planet. Sci. Lett. 174 (1999) 81–97.
[9] C. Hawkesworth, R. George, S. Turner, G. Zellmer, Time scales of magmatic processes, Earth Planet. Sci. Lett. 218 (2004) 1–16.
[10] P. Bachèlery, Le Piton de la Fournaise (Ile de la Réunion). Etude volcanologique, structurale et pétrologique, Thèse, Université de Clermont-Ferrand, (1981) 215.
[11] J.-F. Lénat, P. Bachèlery, Structure et fonctionnement de la zone centrale du Piton de la Fournaise, in: J.-F. Lénat (Ed.), Le volcanisme de la Réunion, Monographie (1990), Centre de Recherches Volcanologiques, Clermont-Ferrand, France, 1990, pp. 257–296.
[12] P.-Y. Gillot, P. Nativel, Eruptive history of the Piton de la Fournaise volcano, Reunion Island, Indian Ocean, J. Volcanol. Geotherm. Res. 36 (1989) 53–65.
[13] T. Staudacher, C.J. Allègre, Ages of the second caldera of Piton de la Fournaise volcano (Réunion) determined by cosmic ray produced ^{3}He and ^{21}Ne, Earth Planet. Sci Lett. 119 (1993) 395–404.
[14] J.-F. Lénat, D. Fitterman, D.B. Jackson, P. Labazuy, Geoelectrical structure of the central zone of Piton de la Fournaise volcano (Réunion), Bull. Volcanol. 62 (2000) 75–89.
[15] T. Staudacher, P. Bachèlery, M. Semet, J.L. Cheminée, et al., Piton de la Fournaise, geophysical portrayal of the March fissure eruptions, Bull. Glob. Volcanism Netw. 23 (1998) 2–5.
[16] B. de Voogd, S.P. Palomé, A. Hirn, P. Charvis, J. Gallart, D. Rousset, J. Danobeitia, H. Perroud, Vertical movements and material transport during hotspot activity: seismic refraction profiling offshore La Réunion, J. Geophys. Res. 104 (1999) 2855–2874.
[17] K. Aki, V. Ferrazzini, Comparison of Mount Etna, Kilauea and Piton de la Fournaise by quantitative modelling of their eruption histories, J. Geophys. Res. 106 (2001) 4091–4102.
[18] K. Aki, V. Ferrazzini, Seismic monitoring of an active volcano for prediction, J. Geophys. Res. 105 (2000) 16617–16640.
[19] D. Graham, J. Lupton, F. Albarède, M. Condomines, A 360,000 year helium isotope record from Piton de la Fournaise, Réunion Island, Nature 347 (1990) 545–548.
[20] F. Albarède, B. Luais, G. Fitton, M.P. Semet, E. Kaminski, B.G.J. Upton, P. Bachèlery, J.L. Cheminée, The geochemical regimes of Piton de la Fournaise volcano (Réunion) during the last 530,000 years, J. Petrol. 38 (1997) 171–201.
[21] H. Bureau, N. Métrich, M.P. Semet, T. Staudacher, Fluid-magma decoupling in a hot spot volcano, Geophys. Res. Lett. 26 (1999) 3501–3504.
[22] I. Vlastélic, T. Staudacher, M. Semet, Rapid change of lava composition from 1998 to 2002 at Piton de la Fournaise (Réunion) inferred from Pb isotopes and trace elements: evidence for variable crustal contamination, J. Petrol. 46 (2005) 79–107.
[23] P. Bachèlery, Evolution structurale des boucliers basaltiques, HDR-Thèse, Université de la Réunion, (1999) 412 pp.
[24] J. Kornprobst, P. Boivin, P. Bachèlery, L'alimentation des éruptions récentes du Piton de la Fournaise (Ile de la Réunion, Océan Indien): degré d'évolution et niveau de ségrégation des laves émises, C. R. Acad. Sci. 288 (1979) 1691–1694.
[25] F. Albarède, V. Tamagnan, Modelling the recent geochemical evolution of the Piton de la Fournaise volcano, Réunion Island, J. Petrol. 29 (1988) 997–1030.
[26] R. Clocchiatti, A. Havette, P. Nativel, Relations pétrogénétiques entre les basaltes transitionnels et les océanites du Piton de la Fournaise (île de la Réunion, Océan Indien) à partir de la composition chimique des inclusions vitreuses des olivines et des spinelles, Bull. Mineral. 102 (1979) 511–525.
[27] B.G.J. Upton, W.J. Wadsworth, Peridotitic and gabbroic rocks associated with the shield-forming lavas of Réunion, Contrib. Mineral. Petrol. 35 (1972) 139–158.
[28] M. Condomines, J.C. Tanguy, G. Kieffer, C.J. Allegre, Magmatic evolution of a volcano studied by ^{230}Th–^{238}U

disequilibrium and trace element systematics: the Etna case, Geochim. Cosmochim. Acta 46 (1982) 1397–1416.
[29] O. Sigmarsson, S. Carn, J.C. Carracedo, Systematics of U-series nuclides in primitive lavas from the 1730–36 eruption on Lanzarote, Canary Island, and implications for the role of garnet pyroxenites during oceanic basalt formation, Earth Planet. Sci. Lett. 162 (1998) 137–151.
[30] O. Sigmarsson, J. Chmeleff, J. Morris, L. Lopez-Escobar, Origin of ^{226}Ra–^{230}Th disequilibria in arc lavas from southern Chile and implications for magma transfer time, Earth Planet. Sci. Lett. 196 (2002) 189–196.
[31] M. Condomines, C. Hémond, C.J. Allègre, U–Th–Ra radioactive disequilibria and magmatic processes, Earth Planet. Sci. Lett. 90 (1988) 243–262.
[32] J.N. Ludden, Magmatic evolution of the basaltic shield volcanoes of Reunion Island, J. Volcanol. Geotherm. Res. 4 (1978) 171–198.
[33] M.R. Fisk, B.G.J. Upton, C.E. Ford, W.M. White, Geochemical and experimental study of the genesis of magmas of Reunion Island, Indian ocean, J. Geophys. Res. 93 (1988) 4933–4950.
[34] J. Blundy, B. Wood, Mineral-melt partitioning of uranium, thorium and their daughters, Uranium-Series Geochemistry, Rev. Mineral. Geochem., vol. 52, 2003, pp. 59–123.
[35] C. Claude-Ivanaj, B. Bourdon, C.J. Allègre, Ra–Th–Sr isotope systematics in Grande Comore Island: a case study of plume–lithosphere interaction, Earth Planet. Sci. Lett. 164 (1998) 99–117.
[36] A. Nercessian, A. Hirn, J.-C. Lépine, M. Sapin, Internal structure of Piton de la Fournaise volcano from seismic wave propagation and earthquake distribution, J. Volcanol. Geotherm. Res. 70 (1996) 123–143.
[37] F. Albarède, Erratum to "residence time analysis of geochemical fluctuations in volcanic series", Geochim. Cosmochim. Acta 59 (1995) 1903.
[38] J.N. Ludden, Eruptive patterns for the volcano Piton de la Fournaise, Reunion Island, J. Volcanol. Geotherm. Res. 2 (1977) 385–395.
[39] J.-F. Lénat, P. Bachèlery, Dynamics of magma transfer at Piton de la Fournaise (Réunion island, Indian ocean), in: C.-Y. King, R. Scarpa (Eds.), Modelling of Volcanic Processes, Fried. Vieweg und Sohn, Brunswick, Germany, 1998, pp. 57–72.
[40] L. Stieltjes, P. Moutou, A statistical and probabilistic study of the historic activity of Piton de la Fournaise, Réunion Island, Indian Ocean, J. Volcanol. Geotherm. Res. 36 (1989) 67–86.
[41] C. Annen, J.-F. Lénat, A. Provost, The long-term growth of volcanic edifices: numerical modelling of the role of dyke intrusion and lava flow emplacement, J. Volcanol. Geotherm. Res. 105 (2001) 263–289.
[42] P.-J. Gauthier, M. Condomines, ^{210}Pb–^{226}Ra radioactive disequilibria in recent lavas and radon degassing: inferences on the magma chamber dynamics at Stromboli and Merapi volcanoes, Earth Planet. Sci. Lett. 172 (1999) 111–126.
[43] M. Stuiver, P.J. Reimer, E. Bard, J.W. Beck, G.S. Burr, K.A. Hughen, B. Kromer, F.G. McCormac, J.V.D. Plicht, M. Spurk, INTCAL98 radiocarbon age calibration 24,000–0 cal BP, Radiocarbon 40 (1998) 1041–1083.
[44] J.-F. Lénat, Structure et dynamique internes d'un volcans basaltique intraplaque océanique: le Piton de la Fournaise (Ile de la Réunion). Thesis. University Clermont II (1987) Clermont-Ferrand, France.